



# Statistical physics modeling of water vapor adsorption isotherm into kernels of dates: Experiments, microscopic interpretation and thermodynamic functions evaluation

Haifa Alyousef<sup>a</sup>, Mohamed Ben Yahia<sup>b,\*</sup>, Fatma Aouaini<sup>a</sup>

<sup>a</sup> Physics Department, Faculty of Science, Princess Nourah Bint Abdulrahman University, Riyadh, Saudi Arabia

<sup>b</sup> Laboratory of Quantum and Statistical Physics, LR18ES18, Faculty of Sciences of Monastir, Tunisia

Received 20 July 2019; accepted 13 November 2019

Available online 21 November 2019

## KEYWORDS

Sorption equilibrium;  
Water activity adsorption;  
Advanced model;  
Van der Waals law;  
Thermodynamic functions

**Abstract** In this paper, water sorption isotherms into date kernels give interesting insights about the sorption mechanism. The equilibrium adsorption data expressing the change in moisture content of date kernels were collected at three different temperatures using the static gravimetric technique. The adsorption isotherm profiles demonstrated that this process was performed via an infinite number of layers. A modified form of the Brunauer, Emmett and Teller (BET) model is obtained based on the use of the real gas law and statistical physics treatment so the interaction between molecules is considered. This advanced model is used to fit experimental isotherms by numerical simulation. The sorption mechanism is theoretically explained by the parameters that could be related to the water adsorption process. Based on fitting results, we find that the number of molecules per site (parameter  $n$ ) has a linear tendency with temperature thanks to the thermal agitation effect. A deeper analysis of adsorption energy demonstrates that the water vapors are physisorbed in the date kernels. Through the exploitation of our model, three classic thermodynamic functions are investigated to interpret the macroscopic aspect of the adsorption mechanism.

© 2019 The Author(s). Published by Elsevier B.V. on behalf of King Saud University. This is an open access article under the CC BY-NC-ND license (<http://creativecommons.org/licenses/by-nc-nd/4.0/>).

## 1. Introduction

Saudi Arabia is one of the first largely produced of date palm in the world. Fruit of the palm (*Phoenix dactylifera* L.) is rich in mineral salts and vitamins (Assirey, 2015) and excellent material for producing refined sugar, concentrated juice, and fermentation products (Booij et al., 1992). The kernels represent 6–15% of the total weight of the date (AbdulQadir et al., 2011). The date kernels are composed of carbohydrates,

\* Corresponding author at: Faculty of Sciences of Monastir, 5000 Monastir, Tunisia.

E-mail address: [ben\\_yahia\\_med@hotmail.fr](mailto:ben_yahia_med@hotmail.fr) (M. Ben Yahia).

Peer review under responsibility of King Saud University.



Production and hosting by Elsevier

dietary fiber, fat, ash and protein. In addition, the antioxidant content in date seed oil (DSO) was found to be similar with olive oil, which can be as a good source of antioxidant in order to fulfill the consumer's requirements (Golshan Tafti et al., 2017). Date seeds, also called pits, kernels, stones or pipes, are a waste product of date processing and packing plants (Abdul Afiq et al., 2013).

Beside the nutrition and health, the kernels of date have many features and uses; For examples as animal feed ingredient (Al Sumri et al., 2016) or turned into non caffeinated coffee by the Arabs or used sometimes as a soil organic additive (Elwathig Mirghani, 2012). As proposed in recent researches, the kernels of date have several amazing medicinal properties. Indeed, they help to prevent kidney and liver against toxicity or damage (Al-Farsi et al., 2005) and it is useful in treating problem in blood related to sugar (Ishurd et al., 2004). Because they are rich in antioxidants, they are used to liver diseases, prevent DNA damage and help to fight various viral infections (Vayalil, 2002).

The study of the shelf life and safety of this product is of fundamental interest (Al-Muhtaseb et al., 2002). In fact this is important for predicting the physical and organic procedures which occur during food storage (Al-Muhtaseb et al., 2004). This factor is related to the water content because the water is the principal component of natural food stuffs. It plays a crucial role in the food process and the chemical process and has a major impact on food reactions and quality. The behavior of a food product is often described by the humid air that surrounds it. The investigation of such a phenomenon in this paper is outlined through the water vapor sorption isotherm which establishes the link between the moisture content (total moisture content) and the water activity at different ranges of temperature (Al-Muhtaseb et al., 2004). The water activity  $a_w$  represents the dynamic part of water inside the food product and it is often used to justify the food satisfaction. It is defined as the ratio of partial pressure ( $p$ ) of water vapor in air pressure and water vapor saturation ( $p_{vs}$ ) in the same temperature (Aouaini et al., 2018). It also explains the availability of water molecules to contribute in physical, chemical, and microbiological reactions.

Experimental and hypothetical researches of the vapor of water associated with foods have been intensified in an attempt to investigate the water behavior (Al-Muhtaseb et al., 2002). In this way, the interpretation of water vapor sorption into date kernels constitutes the principal motivation, because of its vital importance for predicting the stability of food product (Al-Muhtaseb et al., 2004).

Generally, sorption data are usually presented as isotherms (Aranovich and Donohue, 1998) which attract many researchers due to its interesting applications. Several analytical strategies have been developed in the literature in order to characterize the shape of adsorption isotherms. In this issue the classical density functional theory was used by Monson (2012) to understand adsorption/desorption hysteresis for fluids confined in mesoporous materials. The adsorption of halide ions onto single-crystal electrodes was modeled by Koper (1998) using a lattice-gas approach. Isotherm equation applied to lattice gas with rather general lateral interactions was investigated by Medved et al. (2014). They modeled an adsorption of particles on a solid surface at subcritical temperatures. Centres et al. (2011) provide an improved method for the determination of the energetic

topography of the surface from adsorption isotherms. Adsorption on heterogeneous surfaces was also analyzed by following the behavior of surface coverage versus chemical potential (adsorption isotherm) and the differential heat of adsorption as a function of the coverage (Centres et al., 2011). These Previous studies showed that the topography of a given surface can be obtained from the knowledge of the corresponding adsorption isotherm and a reference curve. In this way, the water sorption isotherms can be suitable tools for both predicting shelf life stability and selecting appropriate packaging method. These isotherms give also significant data on the cooperation of portions of date with water vapor. For example, Dural and Hines (1993) developed a theoretical isotherm equation based on multilayer adsorption on heterogeneous surfaces for water vapor food systems. However, this analytical equation and others previous models (Brunauer et al., 1940) are strictly based on empirical or semi-empirical theories. It is difficult to find one equation which gives accurate results throughout the whole range of water activities, and for all types of foods. The novelty of our paper and the progress against recent works is to develop an advanced model expression which provides physico-chemical properties of the date kernels sorption process at the microscopic level.

In this paper, the interpretation of water vapor sorption isotherms of the date kernels at different temperatures is often characterized by the use of the statistical physics formalism (Ben Yahia et al., 2019). This is one of the satisfying ways of describing an activated surface at molecular level (Sellaoui et al., 2018). The use of the statistical physics treatment will allow, firstly, establishing an advanced model expression, and secondly, to better interpret the sorption process at the microscopic state using the physico-chemical parameters (Bouaziz et al., 2019) of the model, which cannot be interpreted by means of empirical methods.

The paper is composed of two parts: The first is dedicated to the measurement of experimental sorption data of water vapor into date kernels using the static gravimetric approach. In the second part, the process of statistical physics is applied to develop the expression of the advanced BET model which leads to a significant characterization of the sorption mechanism.

## 2. Measurement technique of experimental sorption isotherms

The date kernels used in the experiments of the adsorption isotherms were taken from the date fruit 'phoenix dactylifera L.' from the 'Ajwa' selection.

The surface morphology of the kernels of dates before adsorption was examined with a Scanning electron microscopy (SEM) (Fig. 1).

Generally, numerous techniques are accessible for determining water sorption isotherms (Gal et al., 1981). These techniques can be arranged into three classes:

- (1) The gravimetric technique (Wolf et al., 1985) which includes the determination of weight changes. Weight changes can be measured continuously and discontinuously in dynamic or static systems. Continuous methods employ the use of electro-balances or quartz micro balances. In the discontinuous systems which is used in our

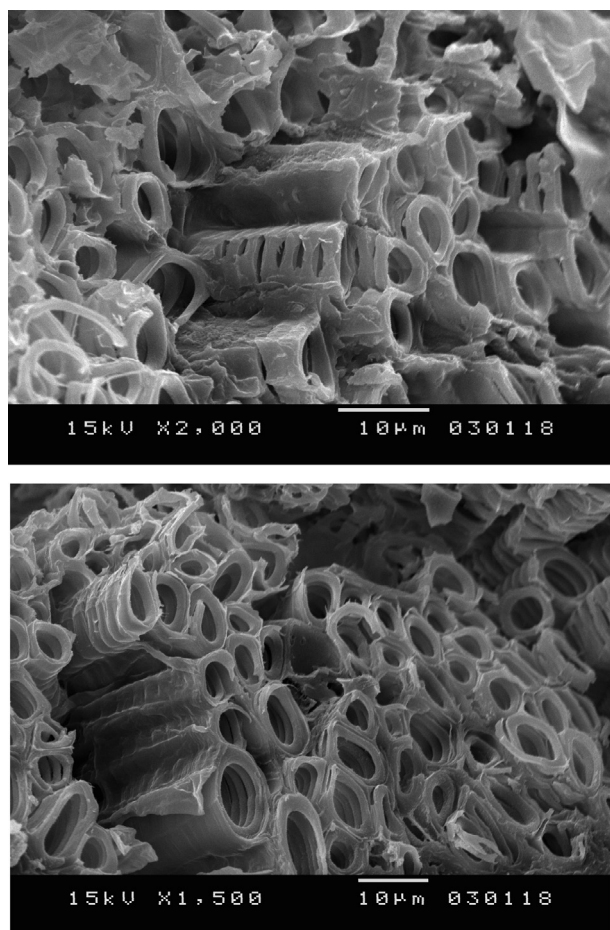


**Fig. 1** Scanning electron microscopy (SEM) images of the Surface morphology of kernel of dates.

experiments, salt or sulphuric acid solutions are placed in vacuum or atmospheric systems with the food material, to give a measure of the equilibrium relative humidity.

- (2) The manometric method (Gal et al., 1981) which measures the vapor pressure of water in the vapor space surrounding the food. The whole system is maintained at constant temperature and the food sample will lose water to equilibrate with the vapour space. This will be indicated by the difference in height on the manometer.
- (3) The hygrometric method (Gal et al., 1981) which measures the equilibrium relative humidity of air in contact with a food material, at given moisture content. Dew-point hygrometers detect the condensation of cooling water vapor. Electric hygrometers measure the change in conductance or capacitance of hygrosensors. Most hygrosensors are coated with a hygroscopic salt, such as LiCl, which absorbs moisture from the food sample.

The adsorption isotherms of the date kernels are determined at 303 K, 313 K and 323 K for a range of water activity varying from 0.0456 to 0.898, using the most helpful technique in these measurements, which is the static gravimetric technique (Bejar et al., 2012). This technique was developed and

standardized in the Water Activity Group of the European COST 90 project (Wolf et al., 1985). We choose to use this experimental technique for its several advantages: (1) Determining the exact dry weight of the sample (Lomauro et al., 1985); (2) Minimizing temperature fluctuation between samples and their surroundings or the source of water vapor (Carbonell et al., 1986); (3) Registering the weight change of the sample in equilibrium with the respective water vapor pressures (Aguerre et al., 1989) and (4) Achieving hygroscopic and thermal equilibrium between samples and water vapor source (Diamante and Murno, 1990).

The experimental setup consists of 11 standard saturated salt solutions which have been used to maintain a regular vapor pressure in a closed space. These salts are LiCl, CaCl<sub>2</sub>, MgCl<sub>2</sub>, Mg(NO<sub>3</sub>)<sub>2</sub>, NaBr, KI, NaNO<sub>3</sub>, NaCl, KCl, BaCl<sub>2</sub> and K<sub>2</sub>SO<sub>4</sub>, and the saturated solutions are obtained by dissolving the necessary amount of salt in distilled water up to super-saturation in order to get  $a_w$  values ranging from 0.1085 to 0.9661. Eleven glass jars with a protective cover are filled to one quarter depth with a prepared salt solution. Then, the containers are placed in a controlled temperature for one day to be stabilized at the analysis temperature.

After that, a tripod is put in each jar to place the date kernel sample in small crucibles (Bahloul et al., 2008). The date kernel samples are placed in the hermetically sealed jars which are then placed in a controlled oven temperature (303, 313 or 323 ± 27.3 K) for equilibration. The samples are weighted every two days using a Mettler AT 400 balance (Boudhrioua et al., 2008). The physical equilibrium is attained when three consecutive weight estimations showed a difference of less than 0.001 g.

The sorption hygroscopic equilibrium of the date kernels is reached in 18 days. The dry mass of the kernels is determined by the exploitation of the vacuum oven drying technique at 378 K for 24 h.

Finally, the equilibrium moisture content is calculated using the following equation:

$$N_a = \frac{m_{eq} - m_d}{m_d} \quad (1)$$

With  $N_a$  (kg water vapour/kg dry matter) being the moisture content,  $m_{eq}$  (kg) being the equilibrium mass and  $m_d$  (kg) being the dried mass.

The experimental isotherms describing the water sorption into the date kernels are illustrated in Fig. 2a.

Firstly, it is noted from Fig. 2a that the adsorbed quantity ( $N_a$ ) decreases by increasing temperature. This fact is explained by the exothermic nature of the adsorption technique which is the normal case of the sorption process. These experimental results need to be interpreted by theoretical explanation.

Moreover, according to the experimental isotherms profiles, the sorption data can be theoretically interpreted by the Guggenheim-Anderson-De Boer (GAB) model (Dural and Hines, 1993); the Brunauer, Emmett and Teller (BET) model (Brunauer et al., 1940), and PELEG model (Peleg, 1993). These analytical models provide an interpretation of multi-layer sorption isotherms with empirical manner. In fact, they provide an estimation of the monolayer value of adsorbed moisture on the surface and the adsorption energy. However, all of them do not provide any physical indication about the adsorption mechanism.

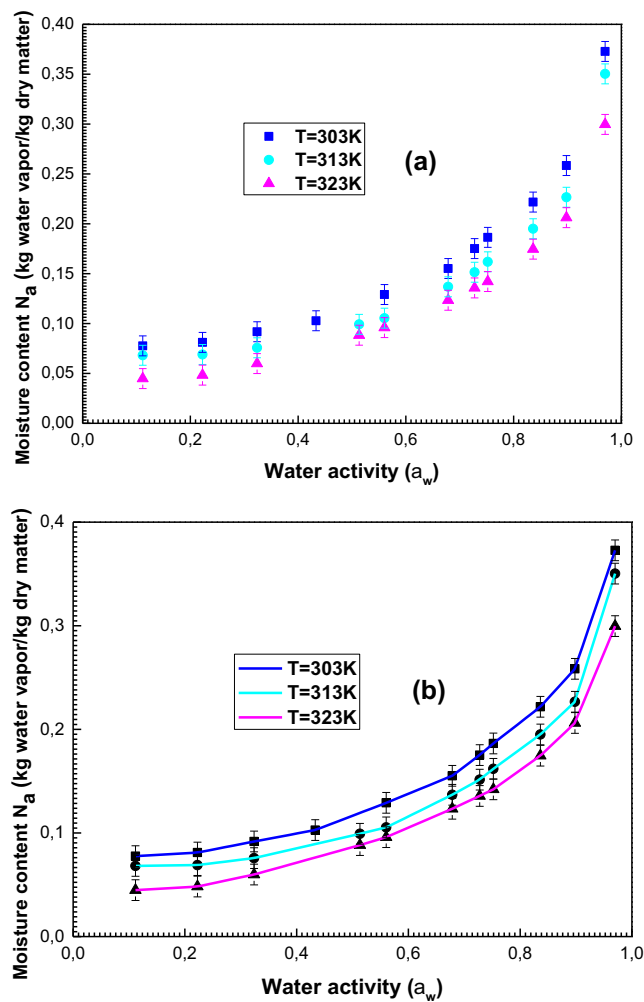


**Fig. 2** (a): Experimental isotherms describing the sorption of water onto kernel of dates, (b): Experimental data simulated with the statistical physics model.

The aim of the next section consists to find an advanced statistical physics model that provides a physical description of the experimental isotherms by the intermediate of the physico-chemical parameters included in its expression.

### 3. Statistical physics modeling

In this theoretical part, we try to develop an analytical expression that gives physical parameters related to the sorption technique. These parameters can facilitate the interpretation of the sorption system at the molecular level.

#### 3.1. Advanced multi-layer model development

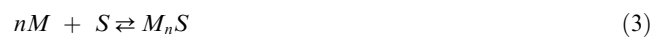
In the literature, one can note that the Brunauer, Emmet and Teller (BET) sorption is based on many hypotheses (Brunauer et al., 1938), whereby it is assumed that an infinite number of layers is adsorbed and that there is no interaction between the adsorbed molecules. The BET expression (Eq. (2)) contains semi-empirical constants (Brunauer et al., 1938):

$$\frac{N_a}{N_0} = \frac{Ca_w}{(1 - a_w)[1 + (C - 1)(a_w)]} \quad (2)$$

With,  $N_a$  is the moisture content (kg/kg dry solid),  $N_0$  is monolayer moisture content (kg/kg dry solid),  $a_w$  is the water activity, and  $C$  is a constant related to the net heat of sorption.

In this work, an advanced form of this model will be developed thanks to the contribution of the statistical physics formalism. This model, called modified BET model, considers the formation of several adsorbed layers and includes intermediate parameters that give physical properties in relationship with the sorption process. Moreover, during our treatment we use the chemical potential of the real gas that takes account of the lateral interactions between molecules in the grand canonical ensemble of Gibbs.

Firstly, it is assumed that the sorption is a process of shifting molecules from the free state to the adsorbed one (Bouaziz et al., 2019). As a result, the equilibrium between the adsorbed phase and the free phase was reached for every experimental measurement. This equilibrium is given by the following equation (Ben Lamine and Bouazra, 1997):



With  $n$  being the maximum number of molecules  $M$  adsorbed by one receptor site  $S$  and  $M_nS$  being the resulting adsorbate-adsorbent complex.

Secondly, we only take into account the translation degrees of freedom since the other degrees act only at an excessive temperature (Nakbi et al., 2018).

The starting point is the partition function of the grand canonical ensemble which is expressed in Eq. (4) (Nakbi et al., 2018):

$$Z_{gc} = \sum_{N_i} e^{-\beta(-\varepsilon_i - \mu)N_i} \quad (4)$$

where  $(-\varepsilon_i)$  is the sorption energy of an adsorbent site  $i$ ,  $\mu$  is the chemical potential of the adsorbed molecule,  $N_i$  is the state of occupation number and  $\beta$  is the Boltzmann's constant.

In our situation, for an infinite multilayer arrangement, it is supposed that one layer is adsorbed with first energy level  $(-\varepsilon_1)$  since it is directly associated with the sorption surface and an infinite number of layers are adsorbed with the second energy  $(-\varepsilon_2)$ . Then, the corresponding partition function can be written as follows (Wjhi et al., 2019):

$$z_{gc} = 1 + e^{\beta(\varepsilon_1 + \mu)} + \sum_{N_i=2}^{\infty} e^{-\beta(-\varepsilon_1 - (N_i - 1)\varepsilon_2 - N_i\mu)} \quad (5)$$

In light of the real gas approach, the chemical potential has the following form (Aouaini et al., 2014):

$$\mu = \mu_p + k_B T \ln \frac{V}{V - Nb} + k_B T \frac{Nb}{V - Nb} - 2a \frac{N}{V} \quad (6)$$

With  $\mu_p$  being the chemical potential of ideal gas,  $V$  being the volume,  $T$  being the temperature,  $N$  being the number of gas molecules,  $k_B$  being the Boltzmann's coefficient ( $1.380648 \times 10^{-23} \text{ JK}^{-1}$ )  $a$  being a constant which is related to the pressure of cohesion and  $b$  describes the covolume of the adsorbate molecule. The idea to use the chemical potential of real gas allows considering the interactions between the molecules.

Assuming that the  $N_M$  adsorbent receptor sites are identical and independent, the average quantity of the occupied adsorbent sites is expressed in Eq. (7) (Ben Lamine and Bouazra, 1997).

$$N_0 = N_M k_B T \frac{\partial \ln(z_{gc})}{\partial \mu} \quad (7)$$

The chemical potential of ideal gas  $\mu_p$  is related to the translational partition function  $z_{tr}$  by the following relation (Nakbi et al., 2018):

$$z_{tr} = V \left( \frac{2\pi m k_B T}{h^2} \right)^{\frac{3}{2}} = N e^{\left( -\frac{\mu_p}{k_B T} \right)} \quad (8)$$

where  $m$  is the mass of an adsorbed molecule,  $V$  is the volume of an individual adsorbate,  $h$  is the constant of Planck ( $6.626 \times 10^{-34}$  J s),  $k_B$  is the Boltzmann coefficient,  $T$  is the temperature and  $N$  is the number of molecules.

Using the same treatment adopted in our previous work (Aouaini et al., 2014), we get the adsorbed quantity of the advanced form of the BET model in Eq. (9).

$$N_a = n \cdot N_0 = n \cdot N_M * \left( \frac{x_1 + x_1 x_2 + \frac{x_1 x_2^2}{1-x_2}}{1 + x_1 - x_2} \right) \quad (9)$$

where

$$x_1 = \left( \frac{a_w}{w_1 (1 - b a_w) e^{2\beta a a_w} e^{-\frac{b a_w}{1 - b a_w}}} \right)^n \quad (10)$$

$$x_2 = \left( \frac{a_w}{w_2 (1 - b a_w) e^{2\beta a a_w} e^{-\frac{b a_w}{1 - b a_w}}} \right)^n \quad (11)$$

with

$$w_1 = e^{-\frac{\Delta E_1^a - \Delta E_v}{RT}} \quad (12)$$

$$w_2 = e^{-\frac{\Delta E_2^a - \Delta E_v}{RT}} \quad (13)$$

where  $(-\Delta E_1^a)$  and  $(-\Delta E_2^a)$  are the molar sorption energies,  $(-\Delta E_v)$  is the saturation vapor energy of the adsorbate molecule,  $R$  is the ideal gas constant ( $8.3144621$  J mol<sup>-1</sup> K<sup>-1</sup>) and  $T$  is the absolute temperature.

The parameters introduced in the previous model are divided into two classes: the first is the steric factor such as the maximum number of adsorbates per site  $n$  and the number of receptor sites  $N_M$ , the second is an energetic one given by  $x_1$  and  $x_2$ .

In the following, the advanced multilayer model is used for the adjustment of the experimental sorption isotherms. The results of fitting are also compared with the BET model given in relation (2).

### 3.2. Numerical adjustment

We use a numerical simulation to fit the experimental results with the theoretical models. The fitting is primarily based on the Levenberg-Marquardt iterating set of rules and the employment of a multivariable non-linear regression.

Three indicators of the goodness of the fit are used as signs of the suit integrity of the experimental data with the proposed models: the coefficient of determination  $R^2$ , the residual root mean square error (RMSE) and the Akaike records criterion (AIC) (Buttry and Ward, 1985).

The results demonstrating that the experimental information is well adjusted through the theoretical model are:  $R^2$  tends to unity, the parameters esteems should fluctuate within  $\pm 3$  RMSE from their exact quantities and the AIC values should be minimum.

Table 1 shows the values of  $R^2$ , RMSE and AIC deduced from the fitting of the experimental isotherms with the two models.

Based on the results in Table 1, we note the following information concerning the variation of these error coefficients: we found that the advanced multi-layer model has the highest  $R^2$  values, which range from 0.97 to 0.99 for all temperatures. We also note that this model has the lowest RMSE and AIC values. Therefore, we adopt the advanced statistical physics model for the theoretical description of the multi-layer sorption of vapor molecules in date kernels.

Fig. 2b illustrates the experimental sorption isotherms simulated with the applied model.

## 4. Interpretation of physico-chemical parameters

The parameters of the adjustment of experimental sorption isotherms by numerical simulation using our model are given in Table 2.

For a better interpretation of the adsorption mechanism, the six physicochemical constants are firstly discussed versus the shapes of the adsorption isotherms and secondly, we interpret their variation as a function of temperature.

### 4.1. Number of molecules consistent with one site 'n'

The parameter  $n$  is an important factor in the sorption phenomenon due to its steric aspect (Knani et al., 2014).

The influence of this steric parameter on the adsorbed quantity can be understood from Fig. 3a.

It is observed that at low water activity, lower values of  $n$  correspond to higher quantities of the adsorbed amount. With the exception of the high value of water activity, the inverse observation is noticed. This can be easily understood through the number of empty receptor sites at the beginning of the sorption process. These sites will attract the adsorbed molecules at low water activity range and therefore the aggregation of the adsorbed molecules on one site is difficult. This gives small values for the parameter  $n$ . At a high-water pressure and particularly close to the saturation, we note the inverse

**Table 1**  $R^2$ , RMSE and AIC values deduced from fitting experimental isotherms with the empirical BET model and with the advanced statistical physics model.

Temperature (K)	303			313			323		
	$R^2$	RMSE	AIC	$R^2$	RMSE	AIC	$R^2$	RMSE	AIC
Empirical BET model	0.89	0.099	9.6	0.92	0.124	10.2	0.91	0.187	8.3
Advanced BET model	0.97	0.026	2.6	0.99	0.064	4.3	0.98	0.046	3.1

**Table 2** Values of the adjusted parameters deduced from the advanced form of the multi-layer model.

Fitting parameters	303 K	313 K	323 K
Number of molecules per site $n$	0.56 ( $\pm 0.015$ )	0.75 ( $\pm 0.02$ )	0.89 ( $\pm 0.02$ )
Density of receptor site $N_M$ (kg/kg)	0.59 ( $\pm 0.021$ )	0.48 ( $\pm 0.017$ )	0.27 ( $\pm 0.013$ )
First energetic parameter $w_1$ (J·mol <sup>-1</sup> )	0.095 ( $\pm 0.009$ )	0.11 ( $\pm 0.006$ )	0.093 ( $\pm 0.003$ )
Second energetic parameter $w_2$ (J·mol <sup>-1</sup> )	0.71 ( $\pm 0.018$ )	0.79 ( $\pm 0.02$ )	0.72 ( $\pm 0.03$ )
Cohesion pressure $a$ (J·mL·mol <sup>-1</sup> )	12.5 ( $\pm 0.3$ ) $10^{-22}$	15.6 ( $\pm 0.34$ ) $10^{-22}$	17.8 ( $\pm 0.299$ ) $10^{-22}$
Covolume $b$ (mL·mol <sup>-1</sup> )	20.11 ( $\pm 0.35$ ) $10^{-9}$	17.9 ( $\pm 0.28$ ) $10^{-9}$	16.2 ( $\pm 0.31$ ) $10^{-9}$

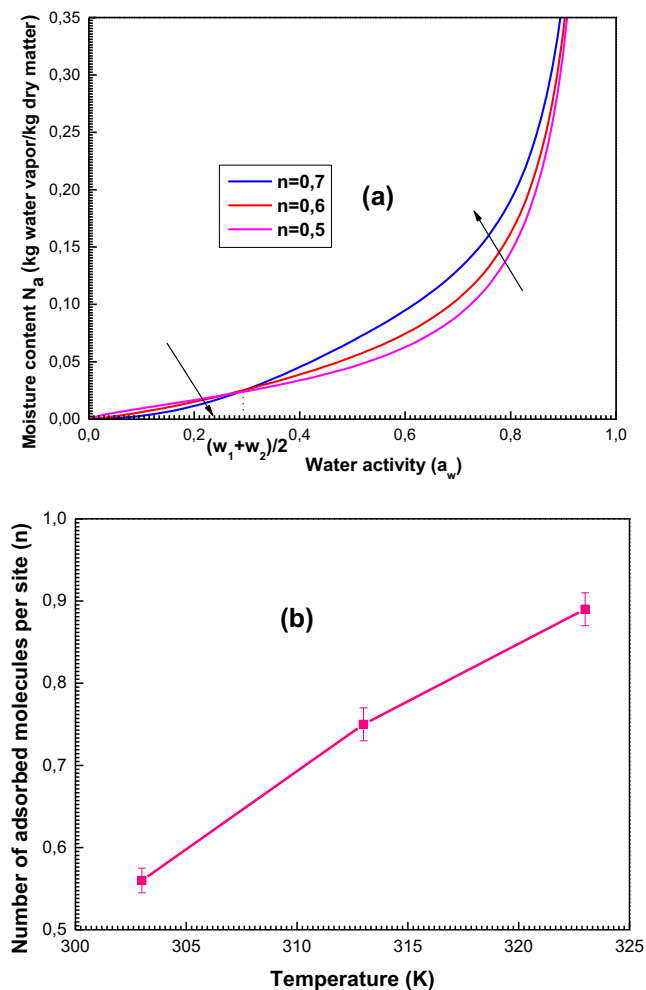


**Fig. 3** Interpretation of the steric parameter number of adsorbed molecules per site  $n$ : (a) Influence of  $n$  on the shapes of sorption isotherms, (b) Evolution of  $n$  as function of temperature.

discover. This is probably attributed to the decrease in the number of empty sites, so the molecules should be aggregated on the receptor sites (highest value of  $n$ ) in order to increase the moisture content.

Fig. 3b depicts the effect of temperature on the fitted stoichiometric constant  $n$ .

We noticed that the increase of temperature caused a rise in the number of molecules per site. This can be probably attributed to the thermal agitation factor (Ben Yahia et al., 2013).

It is known that this parameter conveys the anchorage means of the adsorbate onto the adsorbent as proposed by many authors (Knani et al., 2014). It can be larger or smaller than one. In the case of  $n \geq 1$ , this constant describes the number of adsorbed molecules per site so there is formation of a multi-molecular sorption (Knani et al., 2014). Whereas in the case of  $n \leq 1$ , it represents the portion of the molecule anchored on one site and thus it is a multi-anchorage sorption (Knani et al., 2014). Consequently, we note  $n' = 1/n$  which represents the anchorage number of an adsorbed molecule on several adsorbent sites.

In our case, the fitted values of  $n$  do not exceed 1 and vary between 0.56 and 0.89 for all temperatures. The fact that  $n$  is inferior to 1 shows that no aggregation happens prior to the sorption of water vapor in date kernels and that the adsorption mechanism takes place with a multi-anchorage manner.

#### 4.2. Receptor site density ' $N_M$ '

The parameter  $N_M$  is a steric constant which represents the number of receptor sites per unit of surface (Wjilhi et al., 2019).

We see that an increase in the density of the receptor sites induces an increase in the moisture content (Fig. 4a). It is clear that the rise of the parameter  $N_M$  expands the probability of adsorbate molecules to be captured by the surface of the date kernels.

Fig. 4b depicts the evolution of  $N_M$  versus the adsorption temperatures.

Based on Fig. 4b, we notice that  $N_M$  decreases with temperature. This behavior is described by means of the energy-releasing nature of the sorption system (Bouزيد et al., 2018). This decrease may also be outlined by the steric hindrance during which some sites become hidden by the fact that a set of molecules are adsorbed on one receptor site.

#### 4.3. Interpretation of Van der Waals parameters $a$ and $b$

The parameters  $a$  and  $b$  which are brought in the advanced form of the analytical model using the Van der Waals equation (Ben Yahia et al., 2019), describe the lateral interactions between the adsorbates.

The influence results of the pressure of cohesion  $a$  and the covolume  $b$  at the wet content are given in Fig. 5a and b respectively.

One can see that the smaller the values of  $a$  are, the larger the adsorbed amount is (Fig. 5a). This may be interpreted by the fact that the interaction between the water vapor molecules is weak so the adsorbent-adsorbate interaction becomes excessive.

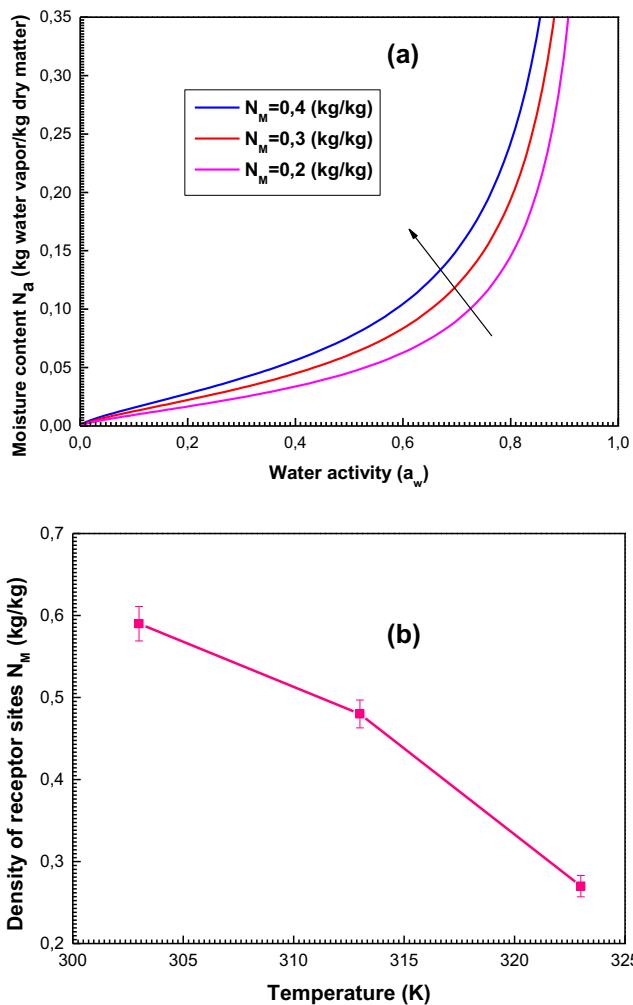


**Fig. 4** Interpretation of the steric parameter density of receptor site  $N_M$ : (a) Influence of  $N_M$  on the shapes of sorption isotherms, (b) Evolution of  $N_M$  as function of temperature.

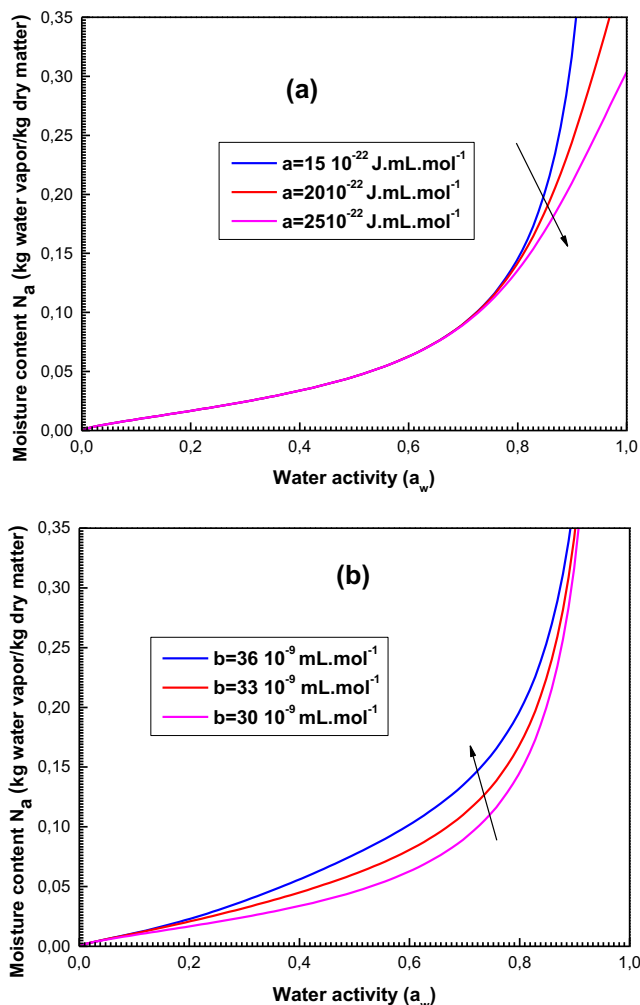
It should be also noted that the impact of  $b$  is opposite to that of  $a$  since the expansion of the covolume  $b$  causes a growth in the adsorbed amount (Fig. 5b). Indeed, with the increase of the value of  $b$ , the adsorbate molecules become more and more distant due to their covolumes, and consequently the attraction between adsorbate molecules becomes weak.

Fig. 6 depicts the evolution of the Van der Waals parameters versus temperatures.

It is observed from this figure that the parameter  $a$  increase by increasing temperature so this parameter acts powerfully at high temperatures. It is also noted that the rise of temperature causes a decrease of the covolume  $b$ . Consequently, we deduce that the sorption is more productive at low temperatures. Thus, the introduction of these two parameters in the expression of the multilayer model plays a crucial role in elucidating the exothermic nature of the sorption mechanism.

#### 4.4. Energetic interpretation: $w_1$ and $w_2$ parameters

The energetic aspect of sorption process is managed by the parameters  $w_1$  and  $w_2$  (Nakhli et al., 2014) which are seen in Eqs. (12) and (13).



**Fig. 5** Influence of the parameters (a) cohesion pressure  $a$  and (b) covolume  $b$  on the shapes of the sorption curves generated by the statistical models.

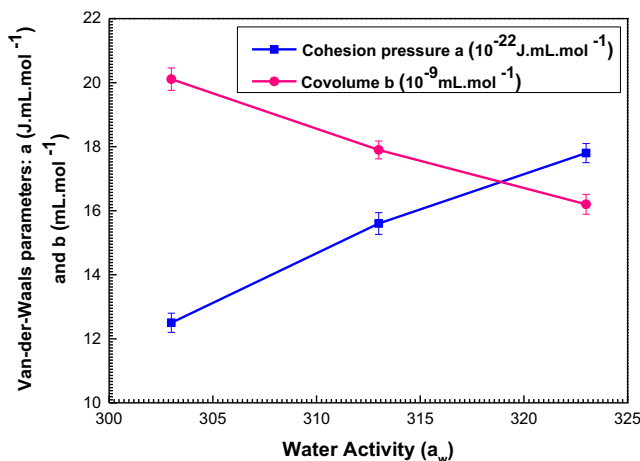


**Fig. 6** Variation of the cohesion pressure  $a$  and the covolume  $b$  versus temperature.

The effect results of these energetic parameters at the sorption isotherms are illustrated in Fig. 7 which depicts the moisture content as a function of  $a_w$  for 3 values of  $w_1$  and  $w_2$ .

We observe from Fig. 7 that  $w_1$  acts on the shape of the sorption data at low water activity and that  $w_2$  intervenes at high values of  $a_w$ . We also notice that the higher the values of  $w_1$  and  $w_2$  are, the lower the moisture content quantity is. This can be easily understood from Eqs. (12) and (13) where we can note that  $w_1$  and  $w_2$  are explicitly related to the sorption energies ( $-\Delta E_1^a$ ) and ( $-\Delta E_2^a$ ) ( $\text{kJ}\cdot\text{mol}^{-1}$ ). The parameters  $w_1$  and  $w_2$  increase as the molar sorption energies decrease in modulus. Therefore, the sorption activity is reduced at high values of  $w_1$  and  $w_2$ .

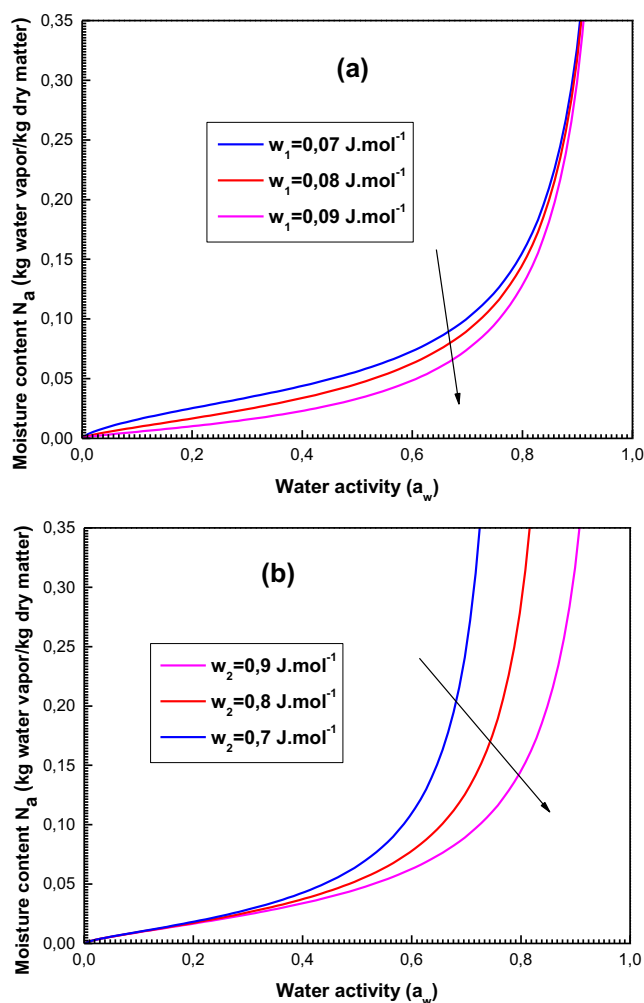


Fig. 7 Effects of the energetic parameters  $w_1$  and  $w_2$  at the sorption isotherms describing the moisture content.

Using the fitting values of  $w_1$  and  $w_2$ , we calculate the adsorption energies of the sorption system as follows (Nakhli et al., 2014):

$$-\Delta E_1^a = -\Delta E_v + RT\ln(w_1) \tag{14}$$

$$-\Delta E_2^a = -\Delta E_v + RT\ln(w_2) \tag{15}$$

The values of the molar sorption energies ( $-\Delta E_1^a$ ) and ( $-\Delta E_2^a$ ) calculated at 303 K, 313 K and 323 K are shown in Table 3.

Fig. 8 depicts the variation of the sorption energies ( $-\Delta E_1^a$ ) and ( $-\Delta E_2^a$ ) versus temperature.

From Table 3 and Fig. 8, one can note three essential results:

- Firstly, the energy ( $-\Delta E_1^a$ ) depicts the cooperation between the water vapor of the primary adsorbed layer and the adsorbent date kernels, i.e. it reflects the adsorbate-adsorbent binding (Ben Yahia et al., 2017). The second energy ( $-\Delta E_2^a$ ) describes the water-water interaction within the multilayer region.

By comparing the results for each temperature, we find that:  $|\Delta E_1^a| > |\Delta E_2^a|$ . This is certainly comprehensible because the adsorbate-adsorbent collaboration is larger than the adsorbates interaction.

- Secondly, Table 3 demonstrates that the calculated sorption energies do not exceed 40 kJ/mol. This suggests that the sorption of water vapor in kernels of dates may be a type of physisorption (Diu et al., 1989). Vander Waals or hydrogen bonds are then basically included.

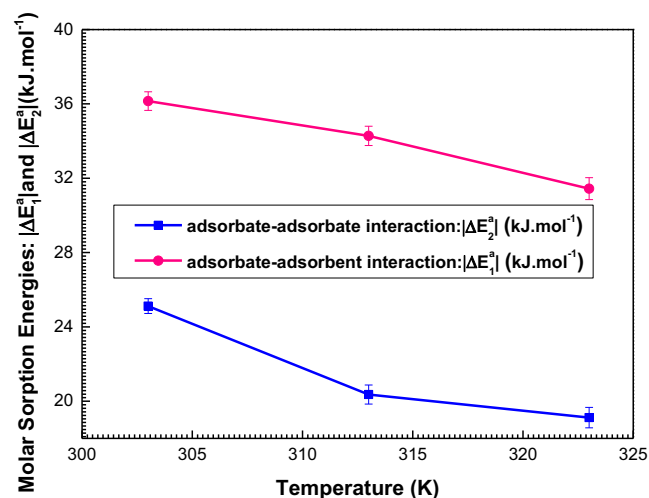


Fig. 8 Temperature dependence of the sorption energies ( $-\Delta E_1$ ) and ( $-\Delta E_2$ ).

Table 3 Values of the molar sorption energies ( $-\Delta E_1$ ) and ( $-\Delta E_2$ ) estimated at 303 K, 313 K and 323 K.

Temperature (K)	303	313	323
$(-\Delta E_1^a)$ ( $\text{kJ}\cdot\text{mol}^{-1}$ )	$-36.15 (\pm 0.5)$	$-34.28 (\pm 0.52)$	$-31.44 (\pm 0.59)$
$(-\Delta E_2^a)$ ( $\text{kJ}\cdot\text{mol}^{-1}$ )	$-25.12 (\pm 0.4)$	$-20.36 (\pm 0.51)$	$-19.12 (\pm 0.55)$

– It may be lastly noticed that an increase of temperature induces a decrease in the sorption energies since the number of receptor sites  $N_M$  decrease with respect to temperature (Fig. 8). Thus, this decrease translates the exothermic criterion of the sorption procedure (Knani et al., 2020).

In the next section, the macroscopic physics interpretation of the sorption system is evaluated by a thermodynamic study according to statistical physics treatment.

## 5. Thermodynamics

Three thermodynamic quantities can be deduced from the advanced BET model, precisely based on the grand canonical partition function.

### 5.1. Configurationally entropy

The interpretation of the entropy is fundamental to depict the behavior of the adsorbed particles at the surface. In this case, the entropy taken into account is the configurationally one.

The value of the sorption entropy is calculated based on the grand potential  $J$  (Couture and Zitoun, 1992), as follows:

$$J = -k_B T \ln Z_{gc} = -\frac{\partial \ln Z_{gc}}{\partial \beta} - TS_a \quad (16)$$

$$TS_a = -\frac{\partial \ln Z_{gc}}{\partial \beta} + k_B T \ln Z_{gc} \quad (17)$$

The entropy is then expressed by:

$$\frac{S_a}{k_B} = -\beta \frac{\partial \ln Z_{gc}}{\partial \beta} + \ln Z_{gc} \quad (18)$$

Subsequently, the sorption entropy  $S_a$  can be expressed as:

$$\frac{S_a}{k_B} = N_M \left[ \left( \frac{x_1 \ln(x_1) + x_1 x_2 \ln(x_2)}{1 + x_1 - x_2} \right) + \ln \left( \frac{1 + x_1 - x_2}{1 - x_2} \right) \right] \quad (19)$$

where  $x_1$  and  $x_2$  are reported in Eqs. (10) and (11).

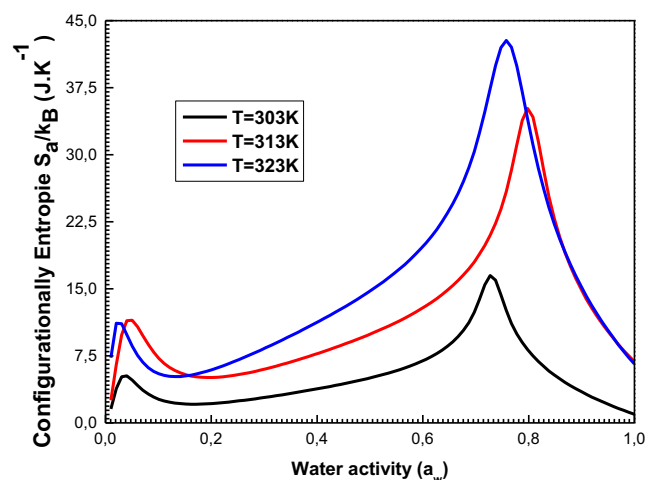


Fig. 9 Development of the Entropy as a feature of water activity at 303, 313, and 323 K.

The profile of the entropy evolution as function of the water activity is given in Fig. 9.

Fig. 9 shows that the entropy extends with the increasing value of  $a_w$  before  $w_1$  and  $w_2$ , and decreases after these particular points. At the beginning, the disorder on the adsorbent surface increases because the adsorbed water vapor has several prospects to find an empty receptor site. After these distinctive points, the adsorbate has an occasional likelihood to choose an adsorbent site due to the surface which tends to the saturation and consequently tends towards being ordered.

One can note that the peak corresponding to  $w_1$  is less than that corresponding to  $w_2$ . This can be explained by the fact that  $w_1$  describes the adsorbate-adsorbent interaction and thus the first peak of the entropy reflects a partial disorder at the level of the first layer. However,  $w_2$  is exposed to the adsorbate-adsorbate interaction within the multilayer region (Yahia et al., 2015). At this point, a whole disorder of the sorption system takes place.

### 5.2. Free sorption enthalpy

In common, any reaction whose variation in free sorption enthalpy  $\Delta G$  is negative should be favorable. As a consequence, its investigation is vital to interpret the physical sorption mechanism. It can be expressed by the following expression (Couture and Zitoun, 1992):

$$G = \mu * N_a \quad (20)$$

$$\frac{G}{k_B T} = n.M_M * \left[ \ln \left( \frac{N}{z_{vr}} \right) + \ln \left( \frac{V}{V - Nb} + \frac{Nb}{V - Nb} - 2a \frac{N}{V k_B T} \right) * \left[ \frac{x_1 + x_1 x_2 + \frac{x_1 x_2^2}{1 - x_2}}{1 + x_1 - x_2} \right] \right] \quad (21)$$

where  $\mu$  is the chemical potential given in Eq. (6).

The calculated values of the enthalpy as a function of the temperature are illustrated in Fig. 10.

We note that the free sorption enthalpy is frequently negative, which suggests that the sorption response is spontaneous (Knani et al., 2020).

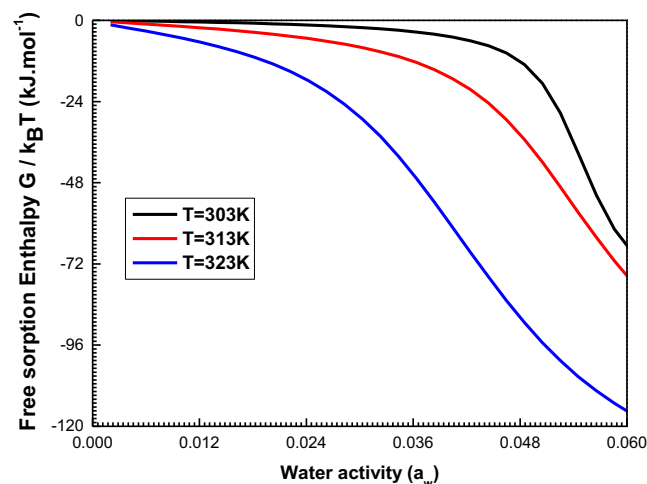
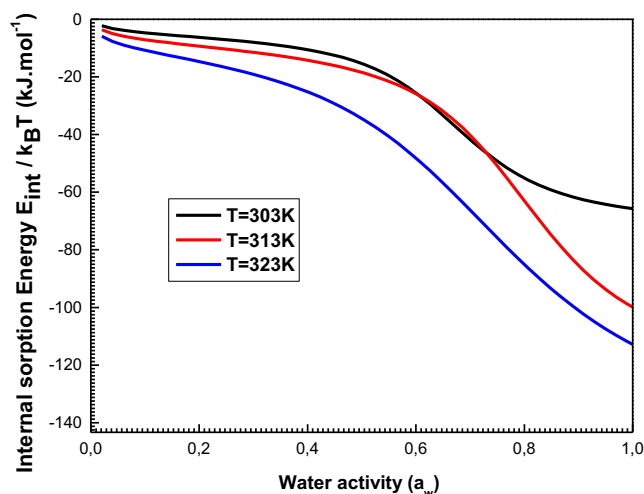


Fig. 10 Evolution of the Gibbs Free Enthalpy at 303, 313, and 323 K.



**Fig. 11** Evolution of the Internal Energy relative to the sorption system at 303, 313, and 323 K.

### 5.3. Internal sorption energy

The investigation of this thermodynamic property specifies the nature of the sorption procedure. Its expression is given in Eq. (22) (Yahia et al., 2015).

$$E_{int} = -\frac{\partial \ln(Z_{gc})}{\partial \beta} + \frac{\mu}{\beta} \left( \frac{\partial \ln(Z_{gc})}{\partial \mu} \right) \quad (22)$$

Using the chemical potential and the partition function, the internal energy is reduced to the following expression:

$$\begin{aligned} \frac{E_{int}}{k_B T} = & -N_M * \left[ \left( \frac{x_1 \ln x_1 + x_1 x_2 \ln x_2}{1 + x_1 - x_2} \right) \right. \\ & + \left( \ln \left( \frac{N}{z_{ir}} \right) + \ln \frac{V}{V - Nb} + \frac{Nb}{V - Nb} - 2a \frac{N}{V k_B T} \right) \\ & * \left. \left( \frac{x_1 + x_1 x_2 + \frac{x_1 x_2^2 \ln x_2}{1 - x_2}}{1 + x_1 - x_2} \right) \right] \quad (23) \end{aligned}$$

All constants and variables of the internal energy expression are mentioned previously.

We illustrate the evolution of the internal sorption energy at 303 K, 313 K, and 323 K in Fig. 11.

We highlight that the internal sorption energy is usually negative for all adsorption temperatures which shows the energy-releasing nature of the sorption process (exothermic phenomenon).

This thermodynamic magnitude has two states of stability which are clearly seen at 303 K: the first partial stable state returns to the saturation of the first layer and the second is the total state of stability after the formation of all the layers of adsorbed molecules (Knani et al., 2020).

## 6. Results discussion

The experimental results showed that the sorption capacity of date kernels decreases as a function of temperature (Fig. 2a). The advanced BET model involved physico-chemical parameters that play a significant role on the explanation of the

behavior of sorption capacity via temperature. We found that the number of molecules linked per adsorbent site ( $n$ ) (Fig. 3b) and the cohesion pressure ( $a$ ) (Fig. 6) increased by increasing temperature. On contrary, the density of receptor sites ( $N_M$ ) (Fig. 4b), the covolume ( $b$ ) (Fig. 6) and the sorption energies ( $(-\Delta E_1^a)$  and  $(-\Delta E_2^a)$ ) (Fig. 8) decreased versus temperature. Based on this finding, it can be established that the number of molecules linked per adsorbent site and the cohesion pressure were not the dominant factor of adsorption process and that the other parameters play a crucial role in elucidating the exothermic nature of the sorption mechanism. It can be also noted that despite the monolayer adsorption capacity is mainly related with the number of molecules linked per adsorbent site and the density of receptor sites ( $N_{mono} = nN_M$ ) it is clear that the trends of these two parameters were totally independent.

In view of thermodynamic part, it was highlighted that the study of internal sorption energy (which is specifically due to the sorption energy) confirms the energy-releasing criterion of date kernels adsorption. Correlating this finding with all parameter trends of the statistical physics model, it was possible to understand that the sorption energies ( $(-\Delta E_1^a)$  and  $(-\Delta E_2^a)$ ) had the most relevant influence on the sorption capacities.

## 7. Conclusion

The purpose of this paper is to provide an evidence for the behavior of the water vapor in date kernels. The use of the grand canonical ensemble applied to statistical physics allowed the development of an advanced theoretical form of the Brunauer, Emmett and Teller (BET) model to describe experimental sorption isotherms. The infinite sorption model seems to be the best way to describe the interaction between the water vapor and the surface of date kernels.

Through the model expression, we determined six physical parameters from the experimental sorption isotherms. The results are mentioned to elucidate the behavior of the parameters versus temperature. We showed that an increase in temperature promotes a rise of the adsorbed molecules per site due to the thermal agitation effect. We found that a rise in temperature caused a decrease of the receptor sites density, which is explained by the exothermic nature of the adsorption process. We also discovered that the sorption is more profitable at low temperature because the cohesion pressure act powerfully at high temperatures. The calculated sorption energies confirm that the binding between the adsorbates and the surface of date kernels occurs with a physisorption process. Looking at the sorption entropy allows noticing that the disorder reached two maximums when the water activity is equal to  $w_1$  and  $w_2$ . An investigation of the free sorption enthalpy and the internal energy demonstrated that the sorption evolves spontaneously and confirmed the exothermic nature of the sorption phenomenon.

## Acknowledgments

This research was funded by the Deanship of Scientific Research at Princess Nourah Bint Abdulrahman University, through the research funding program (Grant No # FRP-1440-10).

## References

- Abdul Afiq, M.J., Abdul Rahman, R., Che Man, B.Y., Al-Kahtani, A. H., Mansor, T.S.T., 2013. Date seed and date seed oil. *Int. Food Res. J.* 20 (5), 2035–2043.
- AbdulQadir, I.M., Garba, I.D., Eiseigbe, E.I., Omofonmwan, E.I., 2011. Nutritional components of Date palm and its production status in Nigeria. *I.J.A.E.R.D.* 4 (2), 83–89.
- Aguerre, R.J., Suarez, C., Viollaz, P.E., 1989. New BET type multilayer sorption isotherms, Part II. *Lebensm-Wiss-Tech.* 22, 192–198.
- Al Sumri, A., Al Siyabi, N., Al Saadi, R., Al Rasbi, S., Al Dalla, A., 2016. Study on the Extraction of Date palm seed oil using Soxhlet Apparatus. *Int. J. Sci. Eng. Res.* 7, 1266–1270.
- Al-Farsi, M., Alasvar, C., Morris, A., Baron, M., Shahidi, F., 2005. Comparison of antioxidant activity, anthocyanins, carotenoids, and phenolics of three native fresh and sun-dried date (*Phoenix dactylifera* L.) varieties grown in Oman. *J. Agric. Food Chem.* 53 (19), 7592–7599.
- Al-Muhtaseb, A.H., McMin, W.A.M., Magee, T.R.A., 2002. Moisture sorption isotherm characteristics of food products: a review. *Trans. Inst. Chem. Eng.* 80, 118–128.
- Al-Muhtaseb, A.H., McMin, W.A.M., Magee, T.R.A., 2004. Water vapor sorption isotherms of starch powders Part 1: mathematical description of experimental data. *J. Food Eng.* 61, 297–307.
- Aouaini, F., Knani, S., Ben Yahia, M., Bahloul, N., Kechaou, N., Ben Lamine, A., 2014. Application of statistical physics on the modeling of water vapor desorption isotherms. *Dry. Tech.* 32, 1905–1922.
- Aouaini, F., Souhail, B., Khemiri, N., Yahia, B.M., Almogait, S.E., AlHarbi, F.F., Almuqrin, H.A., Lamine, B.A., 2018. Study of the CO<sub>2</sub> adsorption isotherms on El Hicha clay by statistical physics treatment: microscopic and macroscopic investigation. *Sep. Sci. Tech.* 54, 2577–2588.
- Aranovich, G., Donohue, M.D., 1998. Analysis of adsorption isotherms: lattice theory predictions, classification of isotherms for gas-solid equilibria, and similarities in gas and liquid adsorption behavior. *J. Colloid Interface Sci.* 200, 273–290.
- Assirey, A.E., 2015. Nutritional composition of fruit of 10 date palm (*Phoenix actylifera* L.). *J. Tai Univ. Sci.* 9, 75–79.
- Bahloul, N., Boudhrioua, N., Kechaou, N., 2008. Moisture desorption-adsorption isotherms and isosteric heats of sorption of Tunisian olive leaves (*Olea europaea* L.). *Indus Crops Pro.* 28, 162–176.
- Bejar, A.K., Mihoubi, N.B., Kechaou, N., 2012. Moisture sorption isotherms-Experimental and mathematical investigations of orange (*Citrus sinensis*) peel and leaves. *Food Chem.* 132, 1728–1735.
- Ben Lamine, A., Bouazra, Y., 1997. Application of statistical thermodynamics to the olfaction-mechanism. *Chem. Sens.* 22, 67–75.
- Ben Yahia, M., Knani, S., Dhaou, H., Hachicha, M.A., Jemni, A., Ben Lamine, A., 2013. Modeling and interpretations by the statistical physics formalism of hydrogen adsorption isotherm on LaNi<sub>4.75</sub>-Fe<sub>0.25</sub>. *Int. J. Hydrogen Ene.* 38, 11536–11542.
- Ben Yahia, M., Knani, S., Hsan, H.B.L., Ben Yahia, M., Nasri, H., Lamine, B.A., 2017. Statistical studies of adsorption isotherms of iron nitrate and iron chloride on a thin layer of porphyrin. *J. Mol. Liq.* 248, 235–245.
- Ben Yahia, M., Yahia, B.M., Aouaini, F., Knani, S., Al-Ghamdi, H., Almogait, S.E., Ben Lamine, A., 2019. Adsorption of sodium and lithium ions onto helicenes molecules: experiments and phenomenological modeling. *J. Mol. Liq.* 288, 110988.
- Booij, I., Piombo, G., Risterucci, M.J., Coupe, M., Thomas, D., Ferry, M., 1992. Study of the chemical-composition of dates at various stages of maturity for varieties characterization of various of date palm cultivars (*Phoenix dactylifera* L.). *Fruit Paris* 47, 667–677.
- Bouaziz, N., Manaa, B.M., Aouaini, F., Lamine, B.A., 2019. Investigation hydrogen adsorption on zeolites A, X and Y using statistical physics formalism. *J. M. Chem. Phys.* 225, 111–121.
- Bouaziz, N., Ben Torkia, Y., Aouaini, F., Nakbi, A., Dhaou, H., Lamine, B.A., 2019. Statistical physics modeling of hydrogen absorption onto LaNi<sub>4.6</sub>Al<sub>0.4</sub>: stereographic and energetic interpretations. *Sep. Sci. Tech.* 54, 2589–2608.
- Boudhrioua, N., Bahloul, N., Kouhila, M., Kechaou, N., 2008. Sorption isotherms and isosteric heats of sorption of olive-leaves (*Chemlali* varietii): experimental and mathematical investigations. *Food Biopro. Proces.* 86, 167–175.
- Bouzid, M., Zhu, Q., Geoff, D.M., Ben Lamine, A., 2018. New insight in adsorption of pyridine on the two modified adsorbents types MN200 and MN500 by means of grand canonical ensemble. *J. Mol. Liq.* 263, 413–421.
- Brunauer, S., Emmett, P.H., Teller, E., 1938. On adsorption of gases in multimolecular layers. *J. Am. Chem. Soc.* 60, 309–319.
- Brunauer, S., Deming, L.S., Teller, E., 1940. On a theory of Van der Waals adsorption of gases. *J. Am. Chem. Soc.* 62, 1723–1732.
- Buttry, A.D., Ward, D.M., 1985. Measurement of interfacial processes at Electrodes Surfaces with onator in contact with liquid. *Ana. Chim. Acta* 175, 99–105.
- Carbonell, J.V., Pinaga, F., Yusa, V., Pena, J.L., 1986. The dehydration of paprika with ambient and heated air and the kinetics of colour dehydration during storage. *J. Food Eng.* 5, 179–192.
- Centres, P.M., Bulnes, F., Zgrablich, G., Ramirez-Pastor, A.J., 2011. Determination of the energetic topography of bivariate heterogeneous surfaces from adsorption isotherms. *Adsorption* 17, 403–410.
- Centres, P.M., Bulnes, F., Riccardo, J.L., Ramirez-Pastor, A.J., Perarnau, M.A., 2011. Adsorption on heterogeneous surfaces with simple topographies. *Adsorpt. Sci. Technol.* 29, 613–627.
- Couture, L., Zitoun, R., 1992. *Physique statistique. Ellipses, Paris.*
- Diamante, L.M., Murno, P.A., 1990. Water desorption isotherms of two varieties of sweet potato. *Int. J. Food Sci. Tech.* 25, 140–156.
- Diu, B., Guthmann, C., Lederer, D., Roulet, B., 1989. *Physique Statistique. Hermann, Paris.*
- Dural, N.H., Hines, A.L., 1993. A new theoretical isotherm equation for water vapor food systems Multilayer adsorption on heterogeneous surfaces. *J. Food. Eng.* 20, 75–96.
- Elwathig Mirghani, M., 2012. Processing of DatePalm Kernel (DPK) for production of nutritious drink. *Aus. J. Basic Appl. Sci.* 6, 22–29.
- Gal, S., 1981. Techniques for obtaining complete sorption isotherms. In: Rockland, L.B., Stewart, G.F. (Eds.), *Water Activity: Influences on Food Quality.* Academic Press, New York, pp. 89–154.
- Golshan Tafti, A., Dahdivan, S.N., Yasini Ardakani, A.S., 2017. Physico-chemical properties and applications of date seed and its oil. *Int. Food Res. J.* 24, 1399–1406.
- Ishurd, O., Zgheel, F., Kermagi, A., Flefla, M., Elmabruk, M., 2004. Antitumor activity of beta-D-glucan from Libyan dates. *J. Med. Food.* 7, 252–255.
- Knani, S., Aouaini, F., Bahloul, N., Khalfaoui, M., Hachicha, A.M., Ben Lamine, A., Kechaou, N., 2014. Modeling of adsorption isotherms of water vapor on Tunisian olive leaves using statistical mechanical formulation. *Physica A* 400, 57–70.
- Knani, S., Khalifa, N., Ben Yahia, M., Aouaini, F., Tounsi, M., 2020. Statistical physics study of the interaction of the 5, 10, 15, 20-tetrakis (4-tolylphenyl) porphyrin (H<sub>2</sub>TTPP) with magnesium ion: New microscopic interpretations. *Arab. J. Chem.* 13, 4374–4385.
- Koper, M.T.M., 1998. A lattice-gas model for halide adsorption on single-crystal electrodes. *J. Electroanal. Chem.* 450, 189–201.
- Lomauro, C.J., Bakshi, A.S., Labuza, T.P., 1985. Evaluation of food moisture sorption isotherm equations. Part I. Fruit, vegetable and meat products. *Lebensm-Wiss-Tech.* 18, 111–117.
- Medved, I., Trnik, A., Cerny, R., 2014. Adsorption isotherm predicted from a lattice gas with general lateral interactions in a single-phase regime. *J. Stat. Mech.*, P12006

- Monson, P.A., 2012. Understanding adsorption/desorption hysteresis for fluids in mesoporous materials using simple molecular models and classical density functional theory. *Micropor. Mesopor. Mater.* 160, 47–66.
- Nakbi, A., Bouzid, M., Ayachi, F., Aouaini, F., Lamine, B.A., 2018. Investigation of caffeine taste mechanism through a statistical physics modeling of caffeine dose-taste response curve by a biological putative caffeine adsorption process in electrophysiological response. *Prog. Biophys. Mol. Bio.* in press.
- Nakhli, A., Bergaoui, M., Khalfaoui, M., Mollmer, J., Moller, A., Ben Lamine, A., 2014. Modeling of high pressure adsorption isotherm using statistical physics approach: lateral interaction of gases adsorption onto metal-organic framework HKUST-1. *Adsorption* 20, 987–997.
- Peleg, M., 1993. Assessment of a semi-empirical four parameter general model for sigmoid moisture sorption isotherms. *J. Food Process Eng.* 16, 21–37.
- Sellaoui, L., Soetaredjo, E.F., Ismadji, S., Petriciolet, B.A., Belver, C., Bedia, J., Lamine, B.A., Erto, A., 2018. Insights on the statistical physics modeling of the adsorption of  $\text{Cd}^{2+}$  and  $\text{Pb}^{2+}$  ions on bentonite-chitosan composite in single and binary systems. *Chem. Eng. J.* 354, 569–576.
- Vayalil, K.P., 2002. Antioxidant and antimutagenic properties of aqueous extract of date fruit (*Phoenix dactylifera* L. *Arecaceae*). *J. Agric. Food Chem.* 50, 610–617.
- Wjihi, S., Peres, C.E., Dotto, L.G., Lamine, B.A., 2019. Physico-chemical assessment of crystal violet adsorption on nano-silica through the infinity multilayer model and sites energy distribution. *J. Mol. Liq.* 280, 58–63.
- Wolf, W., Spiess, W.E.L., Jung, G., 1985. Standardization of isotherm measurements. In: Simatos, D., Multon, J.L. (Eds.), *Properties of Water in Foods*. Martinus Nijhoff, The Netherlands, pp. 661–679.
- Yahia, B.M., Yahia, B.M., Aouaini, F., Ben Lamine, A., 2015. Energetic and thermodynamic analysis of adsorption isotherm type VI of Xenon on graphite nanotubes. *J. Therm. Catal.* 6, 154.